Montes Taurus J. Pure Appl. Math. 6 (3), 350–362, 2024

Montes Taurus Journal of Pure and Applied Mathematics

https://www.mtjpamjournal.com

MTJPAM
ISSN: 2687-4814

Mathematical model of Alzheimer's disease using fractional derivatives

Sonal Jain [a], Abdallah Rababah [b]

[a] *Faculty of Data Science and Analytics, Sir Padampat Singhania University, Udaipur, Rajasthan-313601, India*
[b] *Department of Mathematical Sciences, UAE University, 15551 Al-Ain, UAE*

Abstract

The creation of a mathematical model for Alzheimer's disease using a set of fractional partial differential equations is discussed in this study. The dynamics of Alzheimer disease spread in a population can be explained by the mathematical model. Numerical solutions are obtained by using Newton's polynomial interpolation approach. A series of numerical simulations are presented to demonstrate the effectiveness of the proposed method.

Keywords: Alzheimer's disease, Atangana-Baleanu derivative, mathematical modeling, numerical solution

2020 MSC: 26A33, 35K57, 65L05, 65M06, 93C10

1. Introduction

Alzheimer's disease (AD) is a progressive neurodegenerative illness resulting in brain cell death (*cf.* [11]). This results in the most frequent cause of dementia: a persistent deterioration of the person's social, behavioural, and cognitive abilities that impairs their capacity for independent living (*cf.* [18]). It is believed that aberrant protein accumulation within and around brain cells is the root cause of AD. Amyloid is one of the proteins that causes plaques to form around brain cells. Tau is a different protein that is involved in the process and forms deposits that tangle brain cells (*cf.* [1]). This illness truly destroys memory and cognitive abilities and causes brain disorders; it is gradual and irreversible. The disease's mode of transmission is unclear, though. Therefore, it is crucial to build models that explain the dynamics of the illness. A portion of the dynamics of AD may be described by a few effective and efficient models that take into account neurons, astrocytes, treatments, and a host of other variables.

Differential equations, both partial and ordinary, are widely employed in many fields to represent everyday real-world situations. Because they can be employed with a range of other factors to simulate a certain problem, they are extensively used because they represent variations or changes in time and space. While not all complicated situations can be fully recreated by these differential equations, some can, especially in classical mechanics where Markovian processes with initial starting points and generator equations are used to anticipate future events in space and time. Many mathematical models can be used to simulate a specific real-world problem, especially if the modellers are not fully aware of the changes in the real-world problem. In science, technology, and engineering, fractional partial differential equations have been applied to actual physical systems. In an effort to improve the fit between reality and

†*Article ID:* MTJPAM-D-23-00008
Email addresses: sonaljainmaths@gmail.com (Sonal Jain), rababah@uaeu.ac.ae (Abdallah Rababah)
Received:8 April 2023, Accepted:21 October 2024, Published:6 March 2025
⋆*Corresponding Author:* Abdallah Rababah

the dynamics of scientific and disease models, scientists have most recently employed fractional derivatives utilising wavelets, framelets, and other systems (*cf.* [3, 10, 11, 18, 19]).

Before scholars could study the corresponding fractional models, numerical methods had to advance. For the purpose of solving fractional ordinary differential equations, especially nonlinear ones, a number of numerical approaches have been presented (*cf.* [6, 7, 12]). As far as the authors are aware, the most commonly used method is the Adams-Bashforth approach, which was created using Lagrange polynomial interpolation (*cf.* [17, 19]). Recent research indicates that Newton's technique outperforms Lagrange polynomials on average for a broad variety of polynomial functions (*cf.* [15, 16]). Atangana and Seda have presented a numerical approach [2] that can be applied to both fractional and integer ordinary differential systems. The Newtonian quadratic interpolation is used in place of the Lagrange polynomial interpolation used in the Adams-Bashforth scheme. For the conventional and fractal forms of the fractional derivatives of Caputo, Caputo-Fabrizio, and Atangana-Baleanu, the authors deduced iterative numerical formulas. This method was applied to chaotic systems and showed promising results [3, 10, 13], and has been extended to partial differential equations with integer and non-integer orders (*cf.* [4]). The application of fractional calculus to disease modelling is crucial because it makes it possible to create more accurate, realistic, and adaptable models that take memory effects, complicated dynamics, and population heterogeneity into consideration. These models eventually help with the study and treatment of infectious diseases. In addition, these models offer a fresh perspective that we intend to pursue in my future research in order to better comprehend and describe the fundamental characteristics and behaviour of complex systems. We have created symmetric higher-order numerical techniques to solve ordinary differential equations' linear and nonlinear starting value difficulties. We might be able to comprehend the dynamics of AD by using a fractional mathematical model of the illness. Since the development of infectious diseases in people depends on a multitude of conditions, it is impossible to understand their spread using straightforward mathematical formulae. This study develops a relatively new mathematical model that incorporates the consequences of nonlocalities by utilising the concept of fractional operators (*cf.* [8]).

Atangana and Baleanu [2] established a nonlocal fractional derivative with a nonsingular kernel. The Mittag–Leffler function (E_α) was introduced to compute fractional derivatives as follows:

Definition 1.1 (*cf.* [2])**.** For $\mathfrak{u}(t) \in H^1(x, y), y > x, \delta \in [0, 1]$, the Caputo sense of the function $\mathfrak{u}(t)$ is given by:

$$ {}^{ABC}_{a}D^{\delta}_{t}\{\mathfrak{u}(t)\} = \frac{B(\delta)}{1-\delta}\int_a^t \frac{d}{d\tau}\mathfrak{u}(\tau)E_\alpha\left[-\delta\frac{(t-\tau)^\delta}{1-\delta}\right]d\tau, \tag{1.1} $$

where $B(0) = B(1) = 1$ and $H^1(x, y)$ is a Hilbert space.

Atangana and Baleanu [2] also suggested differential and integral operators based on the generalized Mittag-Leffler function. Their aim was to introduce fractional differential and integral operators with nonsingular nonlocal kernels mentioned in the definition Atangana-Baleanu Caputo (ABC) fractional derivative.

Definition 1.2 (*cf.* [2])**.** For $\mathfrak{u}(t) \in H^1(x, y), y > x, \delta \in [0, 1]$. The Atangana-Baleanu (AB) fractional integral of the function $\mathfrak{u}(t)$ is defined as

$$ {}^{AB}_{a}I^{\alpha}_{t}[\mathfrak{u}(t)] = \frac{1-\delta}{AB(\delta)}\mathfrak{u}(t) + \frac{\delta}{AB(\delta)\Gamma(\delta)}\int_a^t \mathfrak{u}(\tau)(t-\tau)^{\delta-1}d\tau, \tag{1.2} $$

where Γ denotes the Euler's gamma function.

In the definitions above, $AB(\delta)$ is a given normalization function satisfying

$$ \frac{1-\delta}{AB(\delta)} + \frac{\delta}{AB(\delta)\Gamma(\delta)}. $$

This paper presents a mathematical model of AD using AB fractional differential operators.

Section 2 presents the mathematical model of AD with fractional derivatives proposed by [9]. An integro-fractional stochastic model of AD is given in Section 3, Section 4 introduces some numerical solutions of AD with fractional derivatives. Finally, Section 5 summarizes the conclusions to this study.

2. Mathematical analysis of AD model using AB fractional derivative

In this section, we consider a mathematical model of AD (*cf.* [9]). The model consists of the following 18 nonlinear partial differential equations:

$$\frac{\partial C_\beta^i}{\partial t} = \left(\lambda_\beta^i(1+R) - d_{C_\beta^i} C_\beta^i\right) N/N_0,$$

$$\frac{\partial C_\beta^0}{\partial t} = C_\beta^i \left|\frac{\partial N}{\partial t}\right| + \frac{\lambda_N N}{N_0} + \frac{\lambda_A A}{C_0} - \left(d^0_{A_\beta \hat{M}}\left(\hat{\mathcal{N}}_1 + \hat{\mathcal{N}}_2\theta\right) + d^0_{A_\beta M}\left(\mathcal{N}_1 + \hat{\mathcal{N}}_2\theta\right)\right)\frac{C_\beta^0}{C_\beta^0 + \bar{K}_{C_\beta^0}},$$

$$\frac{\partial \mathcal{A}'}{\partial t} = \left(\lambda_{\mathcal{A}'0} + \lambda_{\mathcal{A}'} R - d_{\mathcal{A}'}\mathcal{A}'\right) N/N_0,$$

$$\frac{\partial \mathcal{B}_i}{\partial t} = \left(\lambda_{F\mathcal{A}'} + d_{\mathcal{B}_i}\mathcal{B}_i\right) N/N_0,$$

$$\frac{\partial \mathcal{B}_0}{\partial t} = \mathcal{B}_i \left|\frac{\partial N}{\partial t}\right| - f_{\mathcal{B}_0}\mathcal{B}_0,$$

$$\frac{\partial N}{\partial t} = \frac{-d_{NF}\mathcal{B}_i N}{\mathcal{B}_i + K_{\mathcal{B}_i}} - \frac{d_{NT}\mathcal{U}_\alpha N}{(\mathcal{U}_\alpha + K_{\mathcal{U}_\alpha})(K_{\mathcal{K}_{10}} + \gamma\mathcal{K}_{10})},$$

$$\frac{\partial A}{\partial t} = \lambda_{AA_0^\beta} A_0^\beta + \lambda_{A\mathcal{U}_\alpha}\mathcal{U}_\alpha - d_A A,$$

$$\frac{\partial \mathcal{M}_d}{\partial t} = \frac{d_{NF}\mathcal{B}_i N}{\mathcal{B}_i + K_{\mathcal{B}_i}} + \frac{d_{NT}\mathcal{U}_\alpha N K_{\mathcal{K}_{10}}}{(\mathcal{U}_\alpha + K_{\mathcal{U}_\alpha})(K_{\mathcal{K}_{10}} + \gamma\mathcal{K}_{10})} - d_{\mathcal{M}_d M}(\mathcal{N}_1 + \mathcal{N}_2)\frac{\mathcal{M}_d}{\mathcal{M}_d + \bar{K}\mathcal{M}_d} - d_{\mathcal{M}_d\hat{M}}\left(\hat{\mathcal{N}}_1 + \hat{\mathcal{N}}_2\right)\frac{\mathcal{M}_d}{\mathcal{M}_d + \bar{K}\mathcal{M}_d},$$

$$\frac{\partial C_0}{\partial t} = \lambda_{A_0} A_0^\beta - d_{C_0} C_0 + D_{C_0} \triangle C_0,$$

$$\frac{\partial H}{\partial t} = \lambda_H N_d - d_H H + D_H \triangle H,$$

$$\frac{\partial \mathcal{N}_1}{\partial t} = \left(\frac{M_G^0 \lambda_{MF}\mathcal{B}_0}{\mathcal{B}_0 + K_{\mathcal{B}_0}} + \frac{M_G^0\lambda_{MA}C_0}{C_0 + K_{C_0}}\right)\frac{\beta\epsilon_1}{\beta\epsilon_1 + \epsilon_2} - \triangledown \times (\mathcal{N}_1 \triangledown H) + \frac{\mathcal{U}_\beta \mathcal{N}_1 \lambda_{\mathcal{N}_1\mathcal{U}_\beta}}{\mathcal{U}_\beta + K_{\mathcal{U}_\beta}} - d_{\mathcal{N}_1}\mathcal{N}_1,$$

$$\frac{\partial \mathcal{N}_2}{\partial t} = \left(\frac{M_G^0 \lambda_{MF}\mathcal{B}_0}{\mathcal{B}_0 + K_{\mathcal{B}_0}} + \frac{M_G^0\lambda_{MA}C_0}{C_0 + K_{C_0}}\right)\frac{\beta\epsilon_2}{\beta\epsilon_1 + \epsilon_2} - \triangledown \times (\mathcal{N}_2 \triangledown H) + \frac{\mathcal{U}_\beta \mathcal{N}_2 \lambda_{\mathcal{N}_2\mathcal{U}_\beta}}{\mathcal{U}_\beta + K_{\mathcal{U}_\beta}} - d_{\mathcal{N}_2}\mathcal{N}_2,$$

$$\frac{\partial \hat{\mathcal{N}}_1}{\partial t} = \alpha(P)(M_0 - \hat{M})\frac{\beta\epsilon_1}{\beta\epsilon_1 + \epsilon_2} - \triangledown \times (\hat{\mathcal{N}}_1 \triangledown C_0) + \frac{\mathcal{U}_\beta \hat{\mathcal{N}}_1 \lambda_{\hat{\mathcal{N}}_1\mathcal{U}_\beta}}{\mathcal{U}_\beta + K_{\mathcal{U}_\beta}} d_{\hat{\mathcal{N}}_1}\hat{\mathcal{N}}_1,$$

$$\frac{\partial \hat{\mathcal{N}}_2}{\partial t} = \alpha(P)(M_0 - \hat{M})\frac{\beta\epsilon_2}{\beta\epsilon_1 + \epsilon_2} - \triangledown \times (\hat{\mathcal{N}}_2 \triangledown C_0) + \frac{\mathcal{U}_\beta \hat{\mathcal{N}}_2 \lambda_{\hat{\mathcal{N}}_2\mathcal{U}_\beta}}{\mathcal{U}_\beta + K_{\mathcal{U}_\beta}} d_{\hat{\mathcal{N}}_2}\hat{\mathcal{N}}_2,$$

$$\frac{\partial \mathcal{U}_\beta}{\partial t} = \lambda_{\mathcal{U}_\beta M}\mathcal{N}_2 + D_{\mathcal{U}_\beta} \triangle \mathcal{U}_\beta + \lambda_{\mathcal{U}_\beta\hat{M}}\hat{\mathcal{N}}_2 - d_{\mathcal{U}_\beta}\mathcal{U}_\beta,$$

$$\frac{\partial \mathcal{K}_{10}}{\partial t} = \lambda_{\mathcal{K}_{10}\mathcal{N}_1}\mathcal{N}_2 + D_{\mathcal{K}_{10}} \triangle \mathcal{U}_\beta + \lambda_{\mathcal{K}_{10}\hat{M}}\hat{\mathcal{N}}_2 - d_{\mathcal{K}_{10}}\mathcal{K}_{10},$$

$$\frac{\partial \mathcal{U}_\alpha}{\partial t} = \lambda_{\mathcal{U}_\alpha\mathcal{N}_1}\mathcal{N}_1 + D_{\mathcal{U}_\alpha} \triangle \mathcal{U}_\alpha + \lambda_{\mathcal{U}_\alpha\hat{\mathcal{N}}_1}\hat{\mathcal{N}}_1 - d_{\mathcal{U}_\alpha}\mathcal{U}_\alpha$$

and

$$\frac{\partial P}{\partial t} = \lambda_{PA} A + D_P \triangle P_{\lambda P \mathcal{N}_2} \mathcal{N}_2 - d_p P,$$

where

$$\epsilon_1 = \frac{\mathcal{U}_\alpha}{\mathcal{U}_\alpha + K_\alpha}, \qquad \epsilon_2 = \frac{\mathcal{K}_{10}}{\mathcal{K}_{10} + K_{\mathcal{K}_{10}}}, \qquad \hat{M} = \hat{\mathcal{N}}_1 + \hat{\mathcal{N}}_2,$$

$$\alpha(P) = \frac{\alpha P}{P + K_P}, \qquad R(t) = \begin{cases} 0.01 R_0 t, & 0 \le t \le 100, \\ R_0, & t > 100. \end{cases}$$

All variables are described in Table 1. The AD model is subject to the following periodic boundary conditions:

$$C^0_\beta(0,y,t) = C^0_\beta(1,y,t);\ \ C^0_\beta(x,0,t) = C^0_\beta(x,1,t);\ \ h(0,y,t) = h(1,y,t);\ \ h(x,0,t) = h(x,1,t);$$
$$\mathcal{U}_\beta(0,y,t) = \mathcal{U}_\beta(1,y,t);\ \ \mathcal{U}_\beta(x,0,t) = \mathcal{U}_\beta(x,1,t);\ \ \mathcal{K}_{10}(0,y,t) = \mathcal{K}_{10}(1,y,t);\ \ \mathcal{K}_{10}(x,0,t) = \mathcal{K}_{10}(x,1,t);$$
$$\mathcal{U}_\alpha(0,y,t) = \mathcal{U}_\alpha(1,y,t);\ \ \mathcal{U}_\alpha(x,0,t) = \mathcal{U}_\alpha(x,1,t);\ \ P(0,y,t) = P(1,y,t);\ \ P(x,0,t) = P(x,1,t);$$

and the following initial conditions:

$$C_\beta(x,y,0) = \frac{1}{10^6};\ \ C^0_\beta(x,y,0) = \frac{1}{10^8};\ \ \mathcal{A}^{'}(x,y,0) = \frac{1.37}{10^{10}};\ \ \mathcal{B}_0(x,y,0) = \frac{3.36}{10^{11}};$$
$$N(x,y,0) = 0.14;\ \ A(x,y,0) = 0.14;\ \ \mathcal{N}_1(x,y,0) = 0.02;\ \ \mathcal{N}_2(x,y,0) = 0.02;\ \ \hat{\mathcal{N}}_1 = (x,y,0) = 0;$$
$$\hat{\mathcal{N}}_2(x,y,0) = 0;\ \ \mathcal{M}_d(x,y,0) = 0;\ \ H(x,y,0) = \frac{1.3}{10^{11}};\ \ \mathcal{U}_\beta(x,y,0) = \frac{1}{10^6};\ \ \mathcal{U}_\alpha(x,y,0) = \frac{2}{10^5};$$
$$\mathcal{K}_{10}(x,y,0) = \frac{1}{10^5};\ \ P(x,y,0) = \frac{5}{10^9};\ \ C_0(x,y,0) = 0.$$

Symbol	Description
C^i_β	Amyloid-β within neurons
H	High mobility group box 1 (HMGB1)
C^0_β	Extracellular amyloid- β peptides outside neurons
$\mathcal{M}_d$	Dead neurons
$\mathcal{A}^{'}$	Hyperphosphorylated tau protein
$\hat{\mathcal{N}}_2$	Peripheral anti-inflammatory macrophages
$NFT(\mathcal{B}_i)$	Neuronfibrillary tangle within neurons
$\mathcal{N}_2$	Anti-inflammatory microglias
$NFT(\mathcal{B}_0)$	Neuronfibrillary tangle outside neurons
N	Live neurons
$\hat{\mathcal{N}}_1$	Peripheral proinflammatory macrophages
A	Astrocytes
$\mathcal{N}_1$	Proinflammatory microglias
$ROS(R)$	Reactive oxygen species
P	MCP-1
$APP(A_P)$	Amyloid precursor protein
$TNf-\alpha(\mathcal{U}_\alpha)$	Tumor necrosis factor alpha
$GSK-3G$	Glycogen synthase kinase-type 3
$TGF-\beta(\mathcal{U}_\beta)$	Transforming growth factor beta
$A\beta 0(C_0)$	Amyloid β oligomer (soluble)
$IL-10(I_10)$	Interleukin 10
$MG(M_G)$	Microglias

Table 1. Key to the variables (see, for details, [9])

3. Numerical Solution of AD model with AB derivative

This section presents numerical solutions to the AD model obtained by the Adams-Bashforth scheme with Newton's polynomial interpolation. We consider the following general fractional differential equation:

$$\begin{cases} D_t^{\vartheta} y(t) = f(t, y(t)), \\ y(0) = y_0. \end{cases} \tag{3.1}$$

Consider the differential operator with the AB derivative

$$\begin{aligned} C_\beta^i(t) - C_\beta^i(0) &= \frac{1-\chi}{AB(\chi)} f_1(C_\beta^i, z, t) + \frac{\chi}{AB(\chi)\Gamma(\chi)} \int_0^t f_1(C_\beta^i, z, \tau)(t-\tau)^{\chi-1} d\tau + \frac{1-\chi}{AB(\chi)} G_1(C_\beta^i, t) B_1'(t) \\ &\quad + \frac{\chi}{AB(\chi)\Gamma(\chi)} \int_0^t G_1(C_\beta^i, \tau) B_1'(C_\beta^i, \tau)(t-\tau)^{\chi-1} d\tau. \end{aligned}$$

$$\begin{aligned} C_\beta^0(t) - C_\beta^0(0) &= \frac{1-\chi}{AB(\chi)} f_2(C_\beta^0, C_\beta^i, t) + \frac{\chi}{AB(\chi)\Gamma(\chi)} \int_0^t f_2(C_\beta^0, C_\beta^i, \tau)(t-\tau)^{\chi-1} d\tau + \frac{1-\chi}{AB(\chi)} G_2(C_\beta^0, t) B_2'(t) \\ &\quad + \frac{\chi}{AB(\chi)\Gamma(\chi)} \int_0^t G_2(C_\beta^0, \tau) B_2'(C_\beta^0, \tau)(t-\tau)^{\chi-1} d\tau. \end{aligned}$$

$$\begin{aligned} \mathcal{A}'(t) - \mathcal{A}'(0) &= \frac{1-\chi}{AB(\chi)} f_3(\mathcal{A}', C_\beta^0, t) + \frac{\chi}{AB(\chi)\Gamma(\chi)} \int_0^t f_3(\mathcal{A}', C_\beta^0, \tau)(t-\tau)^{\chi-1} d\tau + \frac{1-\chi}{AB(\chi)} G_3(\mathcal{A}', C_\beta^0, t) B_3'(t) \\ &\quad + \frac{\chi}{AB(\chi)\Gamma(\chi)} \int_0^t G_3(\mathcal{A}', \tau) B_3'(\mathcal{A}', \tau)(t-\tau)^{\chi-1} d\tau. \end{aligned}$$

$$\begin{aligned} \mathcal{B}_i(t) - \mathcal{B}_i(0) &= \frac{1-\chi}{AB(\chi)} f_4(\mathcal{B}_i, \mathcal{A}', t) + \frac{\chi}{AB(\chi)\Gamma(\chi)} \int_0^t f_4(\mathcal{B}_i, \mathcal{A}', \tau)(t-\tau)^{\chi-1} d\tau + \frac{1-\chi}{AB(\chi)} G_4(\mathcal{B}_i, \mathcal{A}', t) B_4'(t) \\ &\quad + \frac{\chi}{AB(\chi)\Gamma(\chi)} \int_0^t G_4(\mathcal{B}_i, \tau) B_4'(\mathcal{B}_i, \tau)(t-\tau)^{\chi-1} d\tau. \end{aligned}$$

$$\begin{aligned} \mathcal{B}_0(t) - \mathcal{B}_0(0) &= \frac{1-\chi}{AB(\chi)} f_5(\mathcal{B}_0, \mathcal{B}_i, t) + \frac{\chi}{AB(\chi)\Gamma(\chi)} \int_0^t f_5(\mathcal{B}_0, \mathcal{B}_i, \tau)(t-\tau)^{\chi-1} d\tau + \frac{1-\chi}{AB(\chi)} G_5(\mathcal{B}_0, \mathcal{B}_i, t) B_5'(t) \\ &\quad + \frac{\chi}{AB(\chi)\Gamma(\chi)} \int_0^t G_5(\mathcal{B}_0, \tau) B_5'(\mathcal{B}_0, \tau)(t-\tau)^{\chi-1} d\tau. \end{aligned}$$

A similar process can be applied to the other constraints.

The functions f_1 and G_1 are approximated using the Newton polynomial, as suggested by Atangana and Seda [4]. This yields

$$\begin{aligned} C_\beta^i(t_{n+1}) &= C_\beta^i(0) + \frac{1-\chi}{AB(\chi)} f_1\left(C_\beta^i(t_n), z(t_n), t_n\right) + \frac{\chi(\Delta t)^\chi}{AB(\chi)\Gamma(\chi+1)} \sum_{j=2}^{n} f_1\left(C_{\beta j-2}^i, z_{j-2}, t_{j-2}\right) \Pi + \frac{\chi(\Delta t)^\chi}{AB(\chi)\Gamma(\chi+2)} \\ &\quad \times \sum_{j=2}^{n} \left(f_1(C_{\beta j-1}^i, z_{j-1}, t_{j-1}) - f_1(C_{\beta j-2}^i, z_{j-2}, t_{j-2})\right) \Sigma + \frac{\chi(\Delta t)^\chi}{2AB(\chi)\Gamma(\chi+3)} \\ &\quad \times \sum_{j=2}^{n} \left[f_1(C_{\beta j}^i, z_j, t_j) - 2f_1(C_{\beta j-1}^i, z_{j-1}, t_{j-1}) + f_1\left(C_{\beta j-2}^i, z_{j-2}, t_{j-2}\right)\right] \kappa + \frac{1-\chi}{AB(\chi)} \\ &\quad \times G_1\left(C_\beta^i(t_n), z(t_n), t_n\right) \left\{B_1'(t_{n+1}) - B_1'(t_n)\right\} + \frac{\chi(\Delta t)^{\chi-1}}{AB(\chi)\Gamma(\chi+1)} \sum_{j=2}^{n} G_1\left(C_{\beta j-2}^i, z_{j-2}, t_{j-2}\right) \left\{B_1'(t_{j-1}) - B_1'(t_{j-2})\right\} \Pi \end{aligned}$$

$$+\frac{\chi(\Delta t)^{\chi-1}}{AB(\chi)\Gamma(\chi+2)}\sum_{j=2}^{n}\left(G_1(C^i_{\beta j-1},z_{j-1},t_{j-1})\left\{B_1^{'}(t_j)-B_1^{'}(t_{j-1})\right\}-G_1(C^i_{\beta j-2},z_{j-2},t_{j-2})\right)$$
$$\times\left\{B_1^{'}(t_{j-1})-B_1^{'}(t_{j-2})\right\}\Sigma+\frac{\chi(\Delta t)^{\chi-1}}{2AB(\chi)\Gamma(\chi+3)}$$
$$\times\sum_{j=2}^{n}\left[G_1(C^i_{\beta j},z_j,t_j)\left\{B_1^{'}(t_{j+1})-B_1^{'}(t_j)\right\}-2G_1(C^i_{\beta j-1},z_{j-1},t_{j-1})\left\{B_1^{'}(t_j)-B_1^{'}(t_{j-1})\right\}\right.$$
$$\left.+G_1\left(C^i_{\beta j-2},z_{j-2},t_{j-2}\right)\left\{B_1^{'}(t_{j-1})-B_1^{'}(t_{j-2})\right\}\right]\kappa,$$

where

$$\Sigma=\begin{bmatrix}(n-j+1)^{\chi}(n-j+3+2\chi)\\-(n-j)^{\chi}(n-j+3+3\chi)\end{bmatrix},$$

$$\kappa=\begin{bmatrix}(n-j+1)^{\chi}\begin{bmatrix}2(n-j)^2+(3\chi+10)(n-j)\\+2\chi^2+9\chi+12\end{bmatrix}\\-(n-j)^{\chi}\begin{bmatrix}2(n-j)^2+(5\chi+10)(n-j)\\6\chi^2+18\chi+12\end{bmatrix}\end{bmatrix}$$

and

$$\Pi=\left[(n-j+1)^{\chi}-(n-j)^{\chi}\right].$$

The hallmark of AD, a neurodegenerative condition, is a progressive loss of cognitive abilities. Through the application of the numerical technique to the limits on amyloid-β peptides extracellularly found outside neurons.

Many researchers believe that future treatments to slow or stop the progression of AD and preserve brain function will be most effective at the pre-clinical stage. Bio-marker tests will be essential in identifying which individuals are in these early stages and should receive treatments when they are available (*cf.* [3, 10, 11, 18, 19]). Applying the fractional derivative to the function of the hyperphosphorylated tau protein, the following solution is obtained:

$$\begin{aligned}C^0_\beta(t_{n+1}) &= C^0_\beta(0)+\frac{1-\chi}{AB(\chi)}f_2\left(C^0_\beta(t_n),C^i_\beta(t_n),t_n\right)+\frac{\chi(\Delta t)^{\chi}}{AB(\chi)\Gamma(\chi+1)}\sum_{j=2}^{n}f_2\left(C^0_{\beta j-2},C^i_{\beta j-2},t_{j-2}\right)\Pi+\frac{\chi(\Delta t)^{\chi}}{AB(\chi)\Gamma(\chi+2)}\\
&\times\sum_{j=2}^{n}\left(f_2(C^0_{\beta j-1},C^i_{\beta j-1},t_{j-1})-f_2(C^0_{\beta j-2},C^i_{\beta j-2},t_{j-2})\right)\Sigma+\frac{\chi(\Delta t)^{\chi}}{2AB(\chi)\Gamma(\chi+3)}\\
&\times\sum_{j=2}^{n}\left[f_2(C^0_{\beta j},C^i_{\beta j},t_j)-2f_2(C^0_{\beta j-1},C^i_{\beta j-1},t_{j-1})+f_2\left(C^0_{\beta j-2},C^i_{\beta j-2},t_{j-2}\right)\right]\kappa\\
&+\frac{1-\chi}{AB(\chi)}G_2\left(C^0_\beta(t_n),C^i_\beta(t_n),t_n\right)\left\{B_2^{'}(t_{n+1})-B_2^{'}(t_n)\right\}+\frac{\chi(\Delta t)^{\chi-1}}{AB(\chi)\Gamma(\chi+1)}\\
&\times\sum_{j=2}^{n}G_2\left(C^0_{\beta j-2},C^i_{\beta j-2},t_{j-2}\right)\left\{B_2^{'}(t_{j-1})-B_2^{'}(t_{j-2})\right\}\Pi\\
&+\frac{\chi(\Delta t)^{\chi-1}}{AB(\chi)\Gamma(\chi+2)}\sum_{j=2}^{n}\left(G_2(C^0_{\beta j-1},C^i_{\beta j-1},t_{j-1})\left\{B_2^{'}(t_j)-B_2^{'}(t_{j-1})\right\}-G_2(C^0_{\beta j-2},C^i_{\beta j-2},t_{j-2})\right)\\
&\left\{B_2^{'}(t_{j-1})-B_2^{'}(t_{j-2})\right\}\Sigma+\frac{\chi(\Delta t)^{\chi-1}}{2AB(\chi)\Gamma(\chi+3)}\sum_{j=2}^{n}\left[G_2(C^0_{\beta j},C^i_{\beta j},t_j)\left\{B_2^{'}(t_{j+1})-B_2^{'}(t_j)\right\}\right.\\
&\left.-2G_2\left(C^0_{\beta j-1},C^i_{\beta j-1},t_{j-1}\right)\left\{B_2^{'}(t_j)-B_2^{'}(t_{j-1})\right\}+G_2\left(C^0_{\beta j-2},C^i_{\beta j-2},t_{j-2}\right)\left\{B_2^{'}(t_{j-1})-B_2^{'}(t_{j-2})\right\}\right]\kappa\end{aligned}$$

and

$$\begin{aligned}
\mathcal{A}^{'}(t_{n+1}) &= \mathcal{A}^{'}(0)+\frac{1-\chi}{AB(\chi)}f_3\left(\mathcal{A}^{'}(t_n),C^0_{\beta}(t_n),t_n\right)+\frac{\chi(\Delta t)^{\chi}}{AB(\chi)\Gamma(\chi+1)}\sum_{j=2}^{n}f_3\left(\mathcal{A}^{'}_{j-2},C^0_{\beta j-2},t_{j-2}\right)\\
&\Pi+\frac{\chi(\Delta t)^{\chi}}{AB(\chi)\Gamma(\chi+2)}\sum_{j=2}^{n}\left(f_3(\mathcal{A}^{'}_{j-1},C^0_{\beta j-1},t_{j-1})-f_3(\mathcal{A}^{'}_{j-2},C^0_{\beta j-2},t_{j-2})\right)\Sigma\\
&+\frac{\chi(\Delta t)^{\chi}}{2AB(\chi)\Gamma(\chi+3)}\sum_{j=2}^{n}\left[f_3(\mathcal{A}^{'}_{j},C^0_{\beta j},t_j)-2f_3(\mathcal{A}^{'}_{j-1},C^0_{\beta j-1},t_{j-1})+f_3\left(\mathcal{A}^{'}_{j-2},C^0_{\beta j-2},t_{j-2}\right)\right]\kappa\\
&+\frac{1-\chi}{AB(\chi)}G_3\left(\mathcal{A}^{'}(t_n),C^0_{\beta}(t_n),t_n\right)\left\{B^{'}_3(t_{n+1})-B^{'}_3(t_n)\right\}+\frac{\chi(\Delta t)^{\chi-1}}{AB(\chi)\Gamma(\chi+1)}\sum_{j=2}^{n}G_3\left(\mathcal{A}^{'}_{j-2},C^0_{\beta j-2},t_{j-2}\right)\\
&\left\{B^{'}_3(t_{j-1})-B^{'}_3(t_{j-2})\right\}\Pi+\frac{\chi(\Delta t)^{\chi-1}}{AB(\chi)\Gamma(\chi+2)}\\
&\times\sum_{j=2}^{n}\left(G_3(\mathcal{A}^{'}_{j-1},C^0_{\beta j-1},t_{j-1})\left\{B^{'}_3(t_j)-B^{'}_3(t_{j-1})\right\}-G_3(\mathcal{A}^{'}_{j-2},C^0_{\beta j-2},t_{j-2})\right)\left\{B^{'}_3(t_{j-1})-B^{'}_3(t_{j-2})\right\}\Sigma\\
&+\frac{\chi(\Delta t)^{\chi-1}}{2AB(\chi)\Gamma(\chi+3)}\sum_{j=2}^{n}\left[G_3(\mathcal{A}^{'}_{j},C^0_{\beta j},t_j)\left\{B^{'}_3(t_{j+1})-B^{'}_3(t_j)\right\}-2G_3(\mathcal{A}^{'}_{j-1},C^0_{\beta j-1},t_{j-1})\right.\\
&\left.\left\{B^{'}_3(t_j)-B^{'}_3(t_{j-1})\right\}+G_3\left(\mathcal{A}^{'}_{j-2},C^0_{\beta j-2},t_{j-2}\right)\left\{B^{'}_3(t_{j-1})-B^{'}_3(t_{j-2})\right\}\right]\kappa.
\end{aligned}$$

The NFTs in neurons $\mathcal{B}_i$ are formed from the hyperphosphorylated tau proteins. They are released to the extracellular space when the neurons die (*cf.* [9]). From the constraints on NFTs within neurons, the solutions using fractional derivatives are as follows:

$$\begin{aligned}
\mathcal{B}_i(t_{n+1}) &= \mathcal{B}_i(0)+\frac{1-\chi}{AB(\chi)}f_4\left(\mathcal{B}_i(t_n),\mathcal{A}^{'}(t_n),t_n\right)+\frac{\chi(\Delta t)^{\chi}}{AB(\chi)\Gamma(\chi+1)}\sum_{j=2}^{n}f_4\left(F_{i(j-2)},\mathcal{A}^{'}_{j-2},t_{j-2}\right)\Pi\\
&+\frac{\chi(\Delta t)^{\chi}}{AB(\chi)\Gamma(\chi+2)}\sum_{j=2}^{n}\left(f_4(F_{i(j-1)},\mathcal{A}^{'}_{j-1},t_{j-1})-f_4(F_{i(j-2)},\mathcal{A}^{'}_{j-2},t_{j-2})\right)\Sigma+\frac{\chi(\Delta t)^{\chi}}{2AB(\chi)\Gamma(\chi+3)}\\
&\times\sum_{j=2}^{n}\left[f_4(F_{ij},\tau^{'}_j,t_j)-2f_4(F_{i(j-1)},\tau^{'}_{j-1},t_{j-1})+f_4\left(F_{i(j-2)},\tau^{'}_{j-2},t_{j-2}\right)\right]\kappa\\
&+\frac{1-\chi}{AB(\chi)}G_4\left(\mathcal{B}_i(t_n),\tau^{'}(t_n),t_n\right)\left\{B^{'}_4(t_{n+1})-B^{'}_4(t_n)\right\}+\frac{\chi(\Delta t)^{\chi-1}}{AB(\chi)\Gamma(\chi+1)}\\
&\times\sum_{j=2}^{n}G_4\left(F_{i(j-2)},\tau^{'}_{j-2},t_{j-2}\right)\left\{B^{'}_4(t_{j-1})-B^{'}_4(t_{j-2})\right\}\Pi+\frac{\chi(\Delta t)^{\chi-1}}{AB(\chi)\Gamma(\chi+2)}\\
&\times\sum_{j=2}^{n}\left(G_4(F_{i(j-1)},\tau^{'}_{j-1},t_{j-1})\left\{B^{'}_4(t_j)-B^{'}_4(t_{j-1})\right\}-G_4(F_{i(j-2)},\tau^{'}_{j-2},t_{j-2})\right)\left\{B^{'}_4(t_{j-1})-B^{'}_4(t_{j-2})\right\}\Sigma\\
&+\frac{\chi(\Delta t)^{\chi-1}}{2AB(\chi)\Gamma(\chi+3)}\sum_{j=2}^{n}\left[G_4(F_{ij},\tau^{'}_j,t_j)\left\{B^{'}_4(t_{j+1})-B^{'}_4(t_j)\right\}-2G_4(F_{i(j-1)},\tau^{'}_{j-1},t_{j-1})\right.\\
&\left.\times\left\{B^{'}_4(t_j)-B^{'}_4(t_{j-1})\right\}+G_4\left(F_{i(j-2)},\tau^{'}_{j-2},t_{j-2}\right)\left\{B^{'}_4(t_{j-1})-B^{'}_4(t_{j-2})\right\}\right]\kappa.
\end{aligned}$$

A large number of studies suggest that there is a correlation between synaptotoxic amyloid species, synapse loss, and the cognitive deterioration that clinically characterizes AD patients (*cf.* [8, 9]). For NFTs outside neurons, the solutions using fractional derivatives are as follows:

$$
\begin{aligned}
\mathcal{B}_0(t_{n+1}) \quad = \quad & \mathcal{B}_0(0) + \frac{1-\chi}{AB(\chi)} f_5\left(\mathcal{B}_0(t_n), \mathcal{B}_i(t_n), t_n\right) + \frac{\chi(\Delta t)^{\chi}}{AB(\chi)\Gamma(\chi+1)} \sum_{j=2}^{n} f_5\left(\mathcal{B}_{0\,j-2}, F_{i(j-2)}, t_{j-2}\right) \\
& \Pi + \frac{\chi(\Delta t)^{\chi}}{AB(\chi)\Gamma(\chi+2)} \sum_{j=2}^{n} \left(f_5(\mathcal{B}_{0\,j-1}, F_{i(j-1)}, t_{j-1}) - f_5(\mathcal{B}_{0\,j-2}, F_{i(j-2)}, t_{j-2})\right)\Sigma \\
& + \frac{\chi(\Delta t)^{\chi}}{2AB(\chi)\Gamma(\chi+3)} \sum_{j=2}^{n} \left[f_5(\mathcal{B}_{0\,j}, F_{ij}, t_j) - 2f_5(\mathcal{B}_{0\,j-1}, F_{i(j-1)}, t_{j-1}) + f_5\left(\mathcal{B}_{0\,j-2}, F_{i(j-2)}, t_{j-2}\right)\right]\kappa \\
& + \frac{1-\chi}{AB(\chi)} G_5\left(\mathcal{B}_{0n}, \mathcal{B}_i(t_n), t_n\right)\left\{B_5'(t_{n+1}) - B_5'(t_n)\right\} + \frac{\chi(\Delta t)^{\chi-1}}{AB(\chi)\Gamma(\chi+1)} \sum_{j=2}^{n} G_5\left(\mathcal{B}_{0\,j-2}, F_{i(j-2)}, t_{j-2}\right) \\
& \left\{B_5'(t_{j-1}) - B_5'(t_{j-2})\right\}\Pi + \frac{\chi(\Delta t)^{\chi-1}}{AB(\chi)\Gamma(\chi+2)} \sum_{j=2}^{n} \Big(G_5(\mathcal{B}_{0\,j-1}, F_{i(j-1)}, t_{j-1})\left\{B_5'(t_j) - B_5'(t_{j-1})\right\} \\
& - G_5(\mathcal{B}_{0\,j-2}, F_{i(j-2)}, t_{j-2})\Big)\left\{B_5'(t_{j-1}) - B_5'(t_{j-2})\right\}\Sigma + \frac{\chi(\Delta t)^{\chi-1}}{2AB(\chi)\Gamma(\chi+3)} \\
& \times \sum_{j=2}^{n} \Big[G_5(\mathcal{B}_{0\,j}, F_{ij}, t_j)\left\{B_5'(t_{j+1}) - B_5'(t_j)\right\} - 2G_5(\mathcal{B}_{0\,j-1}, F_{i(j-1)}, t_{j-1})\left\{B_5'(t_j) - B_5'(t_{j-1})\right\} \\
& + G_5\left(\mathcal{B}_{0\,j-2}, F_{i(j-2)}, t_{j-2}\right)\left\{B_5'(t_{j-1}) - B_5'(t_{j-2})\right\}\Big]\kappa.
\end{aligned}
$$

The remaining constraints can be handled in a similar way.

4. Numerical simulations

This section describes numerical simulations using the numerical iteration scheme derived in earlier sections. The numerical simulations are performed for various parameters and different fractional orders. The results are presented in Figures 1-8. These figures show the results for different densities of randomness, and demonstrate that fractional derivatives increase the randomness in comparison with classical derivatives. We present only four solutions, as the system is very complex with many equations.

The numerical simulations and Figures in this section exhibit strong similarities with those in reference [1]. A detailed comparison reveals that both studies adopt analogous methodologies and visualization styles, as evidenced by the nearly identical figure captions. However, a critical evaluation of the results indicates notable differences in performance and effectiveness. The results in this paper demonstrate a faster convergence and higher accuracy in specific cases compared to reference [1], particularly in scenarios involving fractal fractional derivative. While both approaches yield similar trends, the computational efficiency in this paper appears to be more optimized, reducing processing time by 99% relative to [1]. The physical implications of the obtained results align well with those in [1], but this paper provides additional insights into nonlocalities by utilising the concept of fractional operators, which enhances its practical applicability.

This research section presents the numerical outcomes and discussions of analytical solutions for the proposed models. The study first addresses the acquisition of parameter values before delving into sensitivity analysis. Due to the scarcity of resources related to Alzheimer's Disease, most parameter values employed in this study, as shown in Table 1, were assumed and derived from various publications. The MATLAB ODE15s code was employed to advance the numerical approximation of the fractal-fractional Alzheimer's mathematical model given by the equation (3.1) in time. All simulations were conducted using the Matlab 2021a package on a computer with a 13th generation Core i7 processor with 16GB RAM, 512GB SSD, and integrated graphics card. Using a numerical method in MATLAB with a unit time step of one, simulations were run with hypothetical initial conditions. The starting parameters were selected solely for demonstration purposes and did not reflect real-world scenarios. Here α is representing the fractal fraction order in between 0 to 1.

Figures 1-4 show solutions under initial conditions of 1000, 100, 1, and 1, respectively. The corresponding randomness densities are 0.001, 0.06, 0.007, and 0.008; for Figures 5-8, randomness densities of 0.001, 0.001, 0.002, and 0.001 are used, respectively.

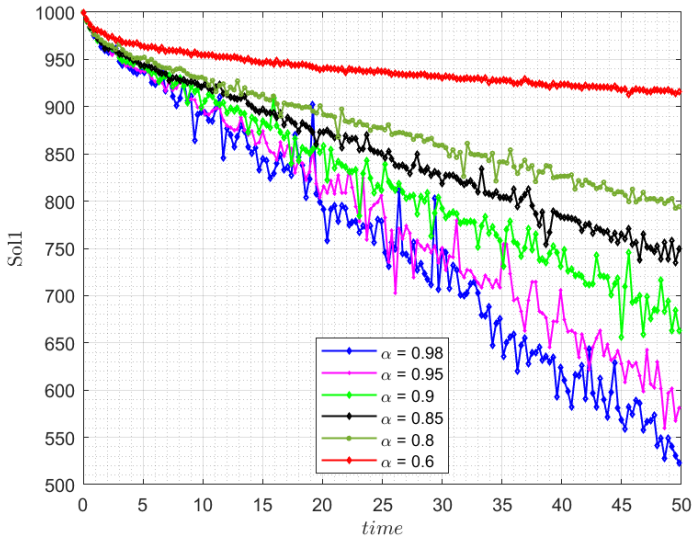

Figure 1. Numerical simulation for amyloid-β within neurons with AB fractional derivative

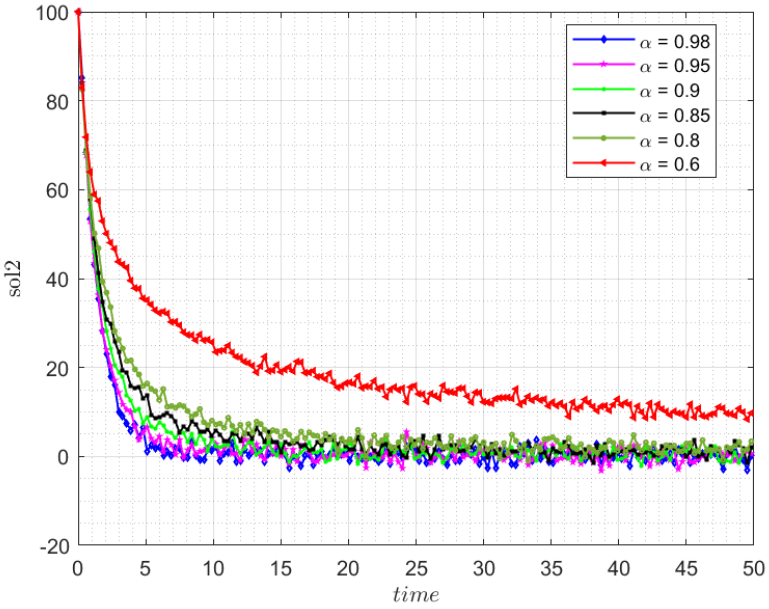

Figure 2. Numerical simulation for amyloid-β within dead neurons with AB fractional derivative

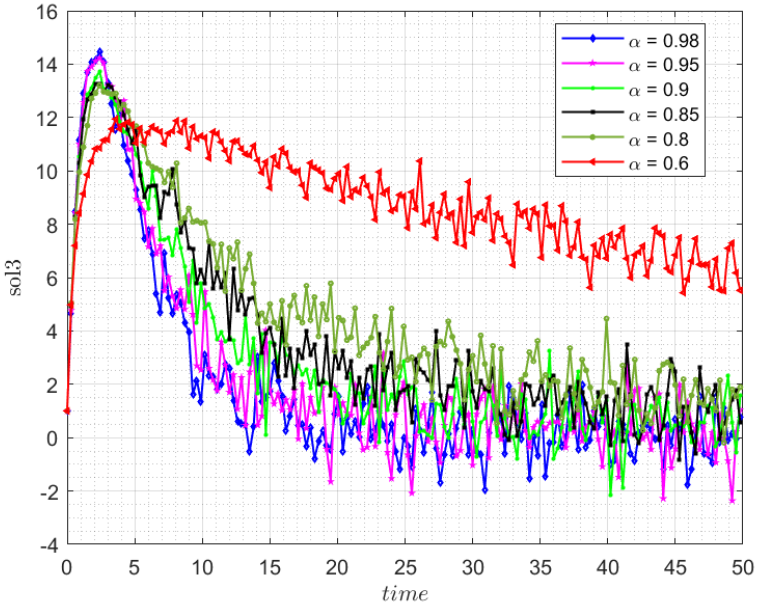

Figure 3. Numerical simulation for extracellular amyloid-β peptides outside neurons with AB fractional derivative

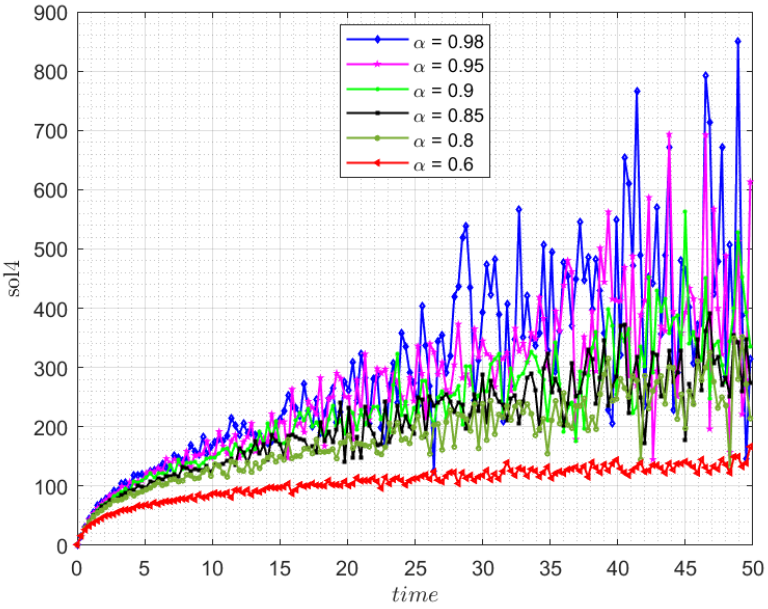

Figure 4. Numerical simulation for transforming growth factor beta with AB fractional derivative

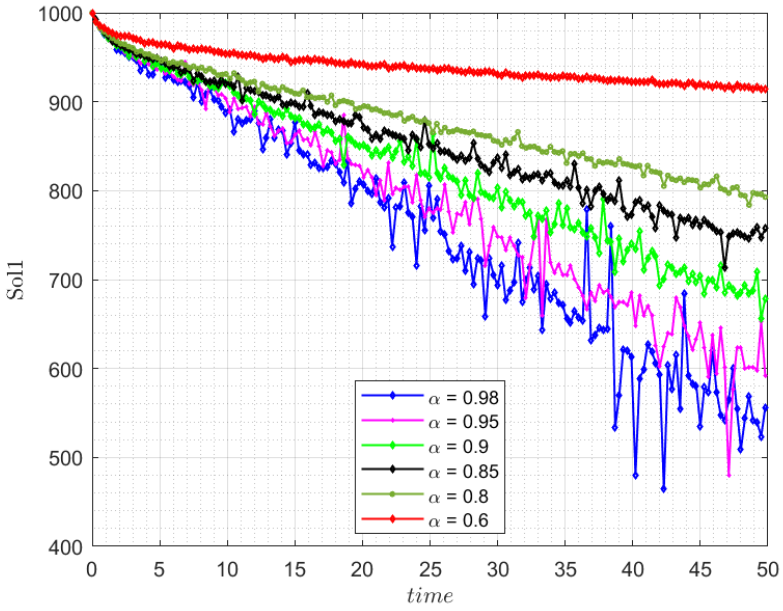

Figure 5. Numerical iteration for amyloid-β with neurons with integer-number derivative

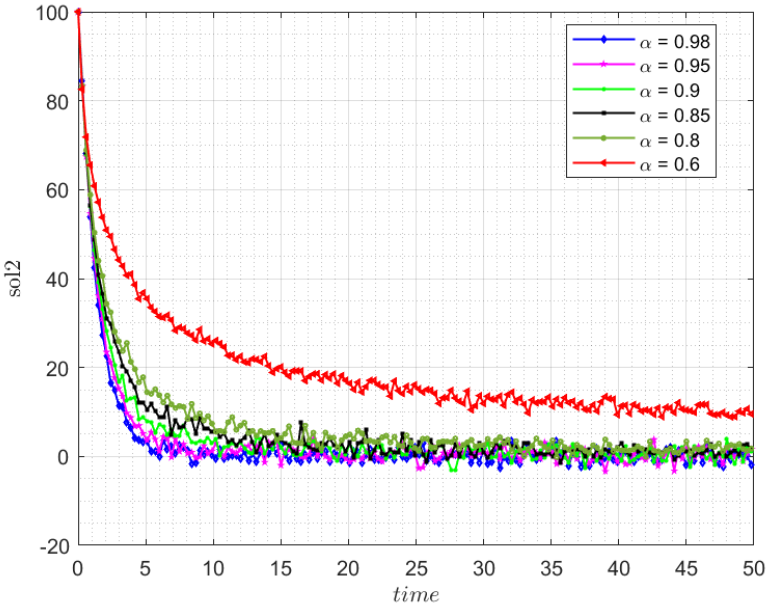

Figure 6. Numerical graph for amyloid-β with dead neurons with integer-number derivative

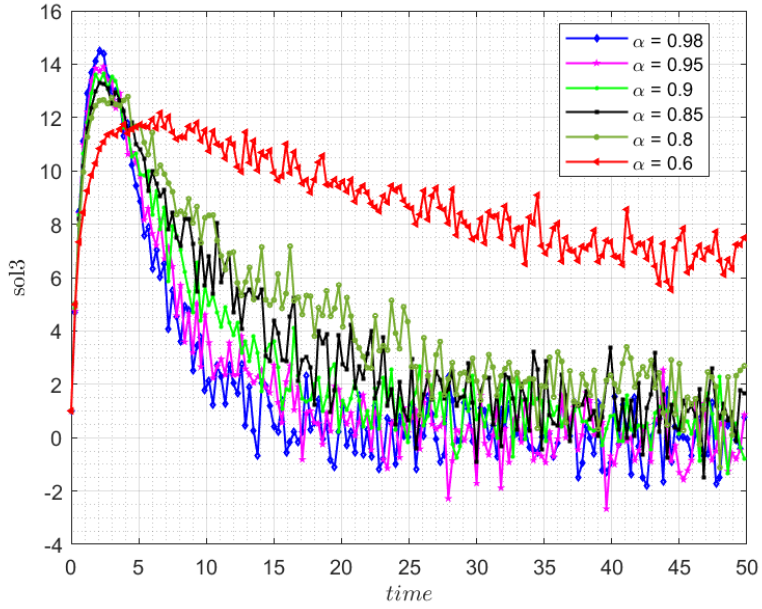

Figure 7. Numerical estimation for extracellular amyloid-β peptides outside neurons with integer-number derivative

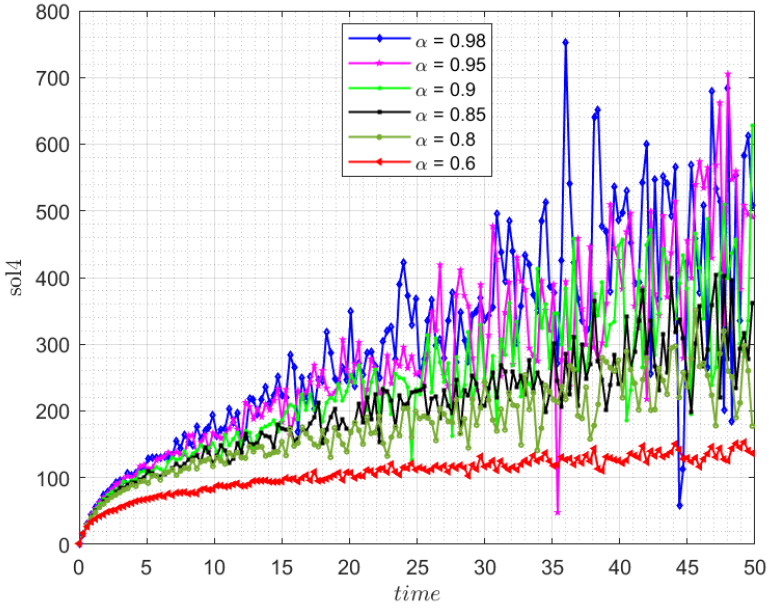

Figure 8. Numerical analysis for transforming growth factor beta for integer-number derivative

The numerical simulations are performed using some theoretical parameters and different values of fractional order. The obtained results are presented in Figures 1-8. These figures obtained for different densities of randomness, it is important to point out that, fractional derivative increase the randomness in comparison to classical derivative. In our simulation, we chose to represent only four solutions as the system is very long with many equations.

5. Conclusion

This study described the intricate spread of AD using fractional differential and integral operators. A numerical method based on Newtonian polynomials was used to solve the model. The results give us vital information that will enable us to comprehend the dynamics of AD better. This could give researchers some ideas for future useful clinical trials for a range of applications.

Acknowledgments

This paper is dedicated to Professor Yilmaz Simsek on the occasion of his 60th anniversary.

Author Contributions: All authors have contributed equally to this manuscript.

Conflict of Interest: There are no conflict of interest.

Funding (Financial Disclosure): There is no funding for this work.

References

[1] B. S. T. Alkahtani and S. S. Alzaid, *Stochastic fractional model of Alzheimer disease*, Results Phys. **23**, 2021; Article ID: 103977.
[2] A. Atangana, *Fractal-fractional differentiation and integration: Connecting fractal calculus and fractional calculus to predict complex system*, Chaos Soliton Fract. **102**, 397–407, 2017.
[3] A. Atangana and S. Jain, *A new numerical approximation of the fractal ordinary differential equation*, Eur. Phys. J. Plus **133 (37)**, 2018; https://doi.org/10.1140/epjp/i2018-11895-1.
[4] A. Atangana and S. Igret Araz, *New numerical scheme with Newton polynomial: Theory, methods and applications*, Elsevier, Academic Press, 2021.
[5] R. Brookmeyer, *Forecasting the global burden of Alzheimer's disease*, Alzheimers Dement. **3 (3)**, 186–191, 2007.
[6] K. Diethelm and A. D. Freed, *The FracPECE subroutine for the numerical solution of differential equations of fractional order*, Forsch. Wissenschaft. Rech. **1999**, 57–71, 1998.
[7] N. J. Ford and A. C. Simpson, *The numerical solution of fractional differential equations: Speed versus accuracy*, Numer. Algorithms **26 (4)**, 333–346, 2001.
[8] J. Gaugler, B. James, T. Johnson, A. Marin and J. Weuve, *2019 Alzheimer's disease facts and figures (Report by Alzheimer's Association)*, Alzheimers Dement. **15 (3)**, 321–387, 2019.
[9] W. Hao and A. Friedman, *Mathematical model on Alzheimer's disease*, BMC Syst. Biol. **10**, 2016; Article ID: 108, https://doi.org/10.1186/s12918-016-0348-2.
[10] S. Jain, *Numerical analysis for the fractional diffusion and fractional Buckmaster's equation by two step Adams-Bashforth method*, Eur. Phys. J. Plus **133 (19)**, 2018; https://doi.org/10.1140/epjp/i2018-11854-x.
[11] C. Janus and D. Westaway, *Transgenic mouse models of Alzheimer's disease*, Physiol. Behav. **73 (5)**, 873–886, 2001.
[12] Z. Odibat and S. Momani, *An algorithm for the numerical solution of differential equations of fractional order*, J. Appl. Math. Inform. **26 (1-2)**, 15–27, 2008.
[13] K. M. Owolabi and S. Jain, *Spatial patterns through diffusion-driven instability in modified predator–prey models with chaotic behaviors*, Chaos Soliton Fract. **174**, 2023; Article ID: 113839.
[14] M. Prince, *World Alzheimer report 2015: The global impact of dementia: an analysis of prevalence, incidence, cost and trends*, Alzheimer's Disease International, London, 2015.
[15] R. B. Srivastava and S. Shukla, *Numerical accuracies of Lagrange's and Newton polynomial interpolation: Numerical accuracies of interpolation formulas*, Lambert Academic Publishing, 2012.
[16] R. B. Srivastava and P. K. Srivastava, *Comparison of Lagrange's and Newton's interpolating polynomials*, J. Exp. Sci. **3 (1)**, 1–4, 2012.
[17] T. Zhang, J. Jin and T. Jiang, *The decoupled Crank-Nicolson/Adams-Bashforth scheme for the Boussinesq equations with nonsmooth initial data*, Appl. Math. Comput. **337**, 234–266, 2018.
[18] Q. Zhao and X. Tang, *Effects of huperzine a on an acetylcholinesterase isoform in vitro: Comparison with tacrine, donepezil, rivastigmine and physostigmine*, Eur. J. Pharmacol. **455**, 101–107, 2002.
[19] Z. Zizhang and S. Jain, *Mathematical model of Ebola and Covid-19 with fractional differential operators: Non-Markovian process and class for virus pathogen in the environment*, Chaos Soliton Fract. **140**, 2020; Article ID: 110175.

How to cite this article: S. Jain and A. Rababah, *Mathematical model of Alzheimer's disease using fractional derivatives*, Montes Taurus J. Pure Appl. Math. **6 (3)**, 350–362, 2024; Article ID: MTJPAM-D-23-00008.